all lung cancer, has become the most common histologic type, largely due to an increase in adenocarcinoma with lepidic growth, which usually shows ground-glass opacity (GGO) (2,3). Lepidic growth is defined as a growth restricted to neoplastic cells along pre-existing alveolar structures, lacking stromal, vascular, or pleural invasion (3). The advance of multislice computed technology has made it possible to detect small GGO nodules that were probably missed when only chest X-ray or thick-section computed tomography (CT) was available. This may partly explain the higher prevalence of adenocarcinoma among lung cancer in recent years (4).

Prognosis and treatment methods for patients with lung cancer depend on the results of histological examination of pulmonary carcinomas (5,6). It is therefore important to predict a likely histological classification of lung cancer with a non-invasive procedure, such as thin-section CT. If the lesion is neoplastic, GGO is related to tumor cell replacement or lepidic growth of the neoplasm. For this reason, GGO has been documented as characteristic of adenocarcinoma (7–14). There are several reports (15–18) on the evaluation of the prevalence of thin-section CT findings for the histology of individual cases of lung cancer, including squamous cell carcinoma, small cell carcinoma, large cell carcinoma, and adenosquamous carcinoma. To the best of our knowledge, however, there are no reports of studies which systematically investigated the prevalence of thin-section CT findings in relation to lung cancer subtypes.

The purpose of this study was to examine if any characteristic thin-section CT findings can predict tumor histology and if such features are related only to tumor size.

Material and Methods

This retrospective study was approved by our institutional review board and written informed consent for CT scans was obtained from all participants.

Subjects

We reviewed the medical and radiological records of patients who had been pathologically diagnosed with lung cancer which had been detected as solitary solid pulmonary nodules (≤3 cm) on thin-section CT at our institution between January 2008 and October 2012. Patients were enrolled only if (a) preoperative, continuous thin-section CT scans of the chest were performed; (b) the nodules were surgically resected; and (c) findings of pathologic examination of the resected lung specimens were available. Histological diagnoses made by a pathologist with 20-year experience in surgical pathology (YT).

CT technology and image analysis

All scans were performed with a 16-slice CT scanner (Aquilion 16; Toshiba, Tokyo, Japan) in helical mode from the apex to the lung base. Technical parameters were: tube voltage, 120 kVp; X-ray tube current, 240–300 mA; rotation speed, 0.5 s; collimation, 1 mm; matrix, 512 × 512; bone reconstruction algorithm. Images were evaluated with the aid of a monitor at a window level of −600 HU and a window width of 1200 HU.

Without knowledge of the histologic diagnosis, two radiologists (BJ and ST, with 5 and 30 years of experience in chest radiology, respectively) independently evaluated the thin-section CT findings including presence or absence of lobulation, coarse spiculation, air bronchogram, cavity, pleural tag, or pleural-based lesion (Fig. 1). The following definitions were used for these findings. Lobulation: irregular undulation of the nodule margin; coarse spiculation: the presence of 2 mm or thicker strands extending from the nodule margin into the lung parenchyma without reaching the pleural surface; air bronchogram: a pattern of air-filled (low-attenuation) bronchi against a background of an opaque (high-attenuation) air-less lung; cavity: an air-filled space, seen as a lucency or low-attenuation area within a pulmonary nodule; pleural tag: as a linear or triangular strand originating from the nodule surface and reaching the pleural surface; pleural-based lesion: a nodule adhering to the pleura and with the diameter of the interface more than half that of the nodule. The final interpretation was based on a consensus of the two radiologists.

Also, both radiologists independently measured the greatest transverse, the shortest transverse, and the vertical diameter of each nodule and calculated the density of lobulation and coarse spiculation, the ratio of the greatest transverse and vertical diameter to the shortest transverse diameter. Density of lobulation (coarse spiculation) was defined as the ratio of lobulation (coarse spiculation) number to the greatest transverse diameter of a nodule. Averaged values of measurements were used for analyses in this study.

Statistical analysis

A kappa or Bland-Altman analysis was performed to assess the inter-observer agreement (19). Chi-square test or Kruskal-Wallis test was used for comparing three groups of data. The discriminant factors for subtypes of lung cancer were examined by means of discriminant analysis. A P value <0.05 was considered to be significant. All of the statistical calculations were performed with SPSS software (PASW Statistics 18; SPSS Inc., Chicago, IL, USA).

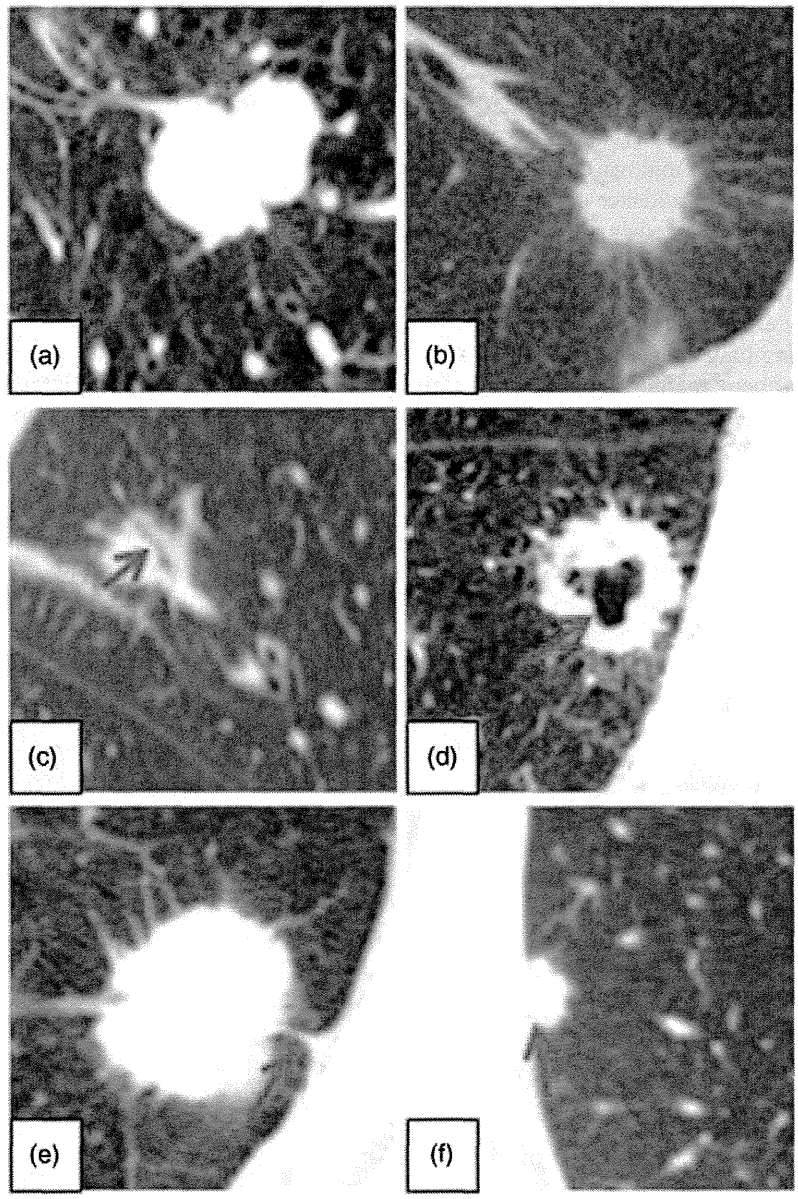

Fig. 1. Thin-section CT findings. (a) Lobulation; (b) coarse spiculation; (c) air bronchogram; (d) cavity; (e) pleural tag; (f) pleural-based lesion.

Results

Between January 2008 and October 2012, 331 patients underwent surgery at our hospital for primary lung cancers consisting of 258 adenocarcinomas, 38 squamous cell carcinomas, 17 small cell carcinomas, three large cell carcinomas, and 15 other lung carcinomas. Thin-section CT scans were available for 164 adenocarcinomas, 33 squamous cell carcinomas, and 17 small cell carcinomas. Of them, 52 nodules with pure GGO and 56 nodules with mixed GGO were excluded. Eventually, 106 solid pulmonary nodules (56 adenocarcinomas, 33 squamous cell carcinomas, and 17 small cell carcinomas) from 106 consecutive patients (76 men and 30 women; mean age, 67 ± 9.5 years) were included in this study.

Agreement between two observers

The kappa values for the two radiologists were 0.61 for lobulation, 0.72 for coarse spiculation, 0.78 for air bronchogram, 0.76 for cavity, 0.90 for pleural tag, and 0.94 for pleural-based lesion, indicating a moderate to excellent agreement (20). The 95% confidence

intervals (CI) of Bland-Altman analysis for the greatest transverse, the vertical, and the shortest transverse diameter were [−2.3, 6.3], [−3.4, 3.9], and [−2.8, 5.3], respectively, which represents an acceptable agreement between the measurements by the two radiologists.

Thin-section CT findings

Comparisons of thin-section CT findings of each histological examination of the lung cancer (Table 1) showed that air bronchogram ($P < 0.01$) was the only significantly different factor. The prevalence of air bronchogram was significantly greater in adenocarcinomas than in squamous cell carcinomas ($P < 0.01$) or small cell carcinomas ($P < 0.01$). The discriminant analysis showed air bronchogram was the discriminant factor for adenocarcinoma of the lung (classification function coefficient: 2.374; $P = 0.001$).

Thin-section CT findings for nodule size (Table 2) showed that, as the tumor increased in size, significant positive linear trends became detectable in the prevalence of lobulation ($P < 0.01$), coarse spiculation ($P < 0.01$) and pleural tag ($P < 0.01$), as well as in the mean values of density of lobulation ($P < 0.01$) and coarse spiculation ($P < 0.01$), while a significant negative linear trend was seen in the ratio of the vertical to the shortest transverse diameter ($P = 0.02$). The prevalence of adenocarcinoma, squamous cell carcinoma, and small cell carcinoma was unrelated to tumor size ($P = 0.224$).

Discussion

Characteristic thin-section CT findings of histology of lung cancer indicated that air bronchogram was the only significant factor for identification of adenocarcinoma in our study. The "air bronchogram" sign is a pattern of air-filled (low-attenuation) bronchi against a background of opaque (high-attenuation) airless lung (21). This sign can be seen in both benign and malignant lesions but shows a preference for malignancy (22).

Pathologically, lung cancer originates from the bronchial epithelium and has two major growth types: a replacement tumor growth of alveolar lining cells, and a compressive or destructive tumor growth (23). In the compressive or destructive growth type, tumor cells with a substantial proliferation and accumulation shape the endobronchial tumor tissue and this causes occlusion of the bronchus. In the replacement growth type, tumor cells creep outward and extend by way of alveolar pores along the alveolar wall and alveolar septa, eventually producing the air bronchogram sign. Therefore, air bronchogram can be seen more often in tumors with predominant replacement or lepidic growth than in tumors with predominant expansive growth (Fig. 2).

Several articles (24–26) have focused on the clinical aspects of air bronchogram and confirmed this sign was characteristic of adenocarcinoma. For example, Kuriyama et al. studied 40 nodules, 20 adenocarcinomas, and 20 benign lesions, with a diameter of <2 cm and found that the prevalence of air bronchogram was 65% in adenocarcinomas but only 5% in benign lesions (24). They concluded the air bronchogram sign in a lung nodule was useful for differentiating adenocarcinomas from benign lesions. However, size of their sample was only half of ours, and they only compared adenocarcinomas with benign lesions, thus excluding other types of lung cancer.

Table 1. Relationship between thin-section CT findings and tumor histology.

	Adenocarcinoma ($n = 56$)	Squamous cell carcinoma ($n = 33$)	Small cell carcinoma ($n = 17$)	*P* value
Prevalence (%)				
Lobulation	68%	85%	82%	0.153
Coarse spiculation	45%	45%	47%	0.984
Air bronchogram	29%	3%	0%	0.001
Cavity	21%	30%	6%	0.139
Pleural tag	63%	52%	53%	0.548
Pleural-based lesion	30%	24%	18%	0.549
Measurement (mean ± SD)				
Density of lobulation	0.21 ± 0.18	0.25 ± 0.18	0.23 ± 0.16	0.634
Density of coarse spiculation	0.06 ± 0.09	0.05 ± 0.07	0.06 ± 0.07	0.638
Ratio of the greatest to the shortest transverse	1.31 ± 0.28	1.26 ± 0.21	1.21 ± 0.13	0.257
Ratio of vertical to the shortest transverse	1.33 ± 0.42	1.19 ± 0.25	1.14 ± 0.32	0.107

In addition, characteristic thin-section CT findings have also been explored for other histological studies of lung cancer with a limited number of patients (only 12–27 patients in each study) (15–18). According to these reports, the prevalence of lobulation, coarse spiculation, cavity, pleural indentation, and air bronchogram varied in squamous cell carcinoma, small and large cell carcinoma, and adenosquamous carcinoma. However, the prevalence of thin-section CT findings based on lung cancer subtypes was not investigated systematically in these studies.

Thin-section CT findings for nodule size in our study showed a significant positive linear trend in the prevalence of lobulation, coarse spiculation, pleural tag, or density of notch and coarse spiculation, but a negative linear trend in the ratio of vertical to the shortest transverse diameter. As far as we know, there is nothing in the literature about this finding.

Tumor cells feature heterogeneous differentiation and growth rates in the margin of the tumor, which is surrounded by heterogeneous tissue structures. As the tumor cells grow, the heterogeneity of the micro-environment within and around the tumor becomes more and more significant, resulting in an increase in the prevalence of lobulation (27). In addition, due to a desmoplastic response, coarse fibrotic strands radiating from the tumor margin invade the lung and form coarse spiculation or pleural tag. This phenomenon may also be secondary to direct tumor extension along interstitial planes or a consequence of lymphangitic spread of the tumor (28). With the tumor enlargement resulting in a more manifest response, the prevalence of observed coarse spiculation and pleural tag increases. Density of lobulation and coarse spiculation can share the same principle with the lobulation and coarse spiculation. The gradual changes in the ratio of the vertical to the shortest transverse diameter indicate that the tumor is becoming rounder as it grows. Although coarse spiculation was reported to be related to the risk of malignancy (29), it was found to be unrelated to lung cancer subtypes in this study.

Our study demonstrated that thin-section CT was useful for histologically distinguishing adenocarcinoma from other peripheral solid lung cancer because the

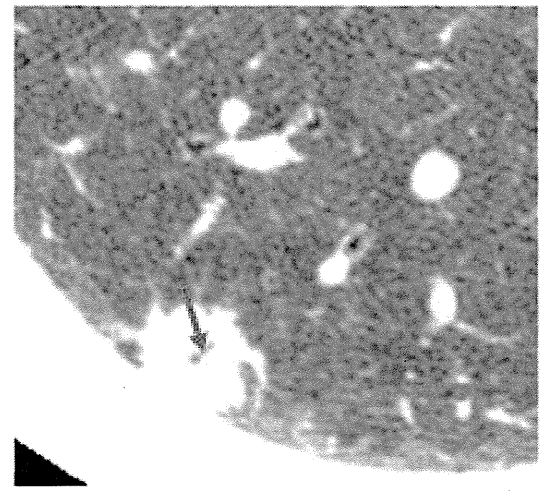

Fig. 2. Adenocarcinoma with air bronchogram in a 65-year-old woman. Thin-section CT demonstrated a solid nodule of 15 mm with air bronchogram (arrow). Pathology confirmed it was non-mucinous minimally invasive adenocarcinoma without lymphatic or vascular invasion.

Table 2. Relationship between thin-section CT findings and tumor size.

	≤1.0 cm ($n=9$)	>1.0 cm and ≤2.0 cm ($n=59$)	>2.0 cm and ≤3.0 cm ($n=38$)	*P* value
Prevalence (%)				
Lobulation	23%	68%	100%	<0.001
Coarse spiculation	11%	31%	76%	<0.001
Air bronchogram	0%	24%	8%	0.045
Cavity	11%	25%	18%	0.518
Pleural tag	44%	49%	74%	0.041
Pleural-based lesion	11%	27%	29%	0.542
Measurement (mean ± SD)				
Density of lobulation	0.05 ± 0.09	0.18 ± 0.18	0.33 ± 0.18	<0.001
Density of coarse spiculation	0.02 ± 0.07	0.04 ± 0.07	0.10 ± 0.09	<0.001
Ratio of the greatest to the shortest transverse	1.24 ± 0.09	1.33 ± 0.32	1.23 ± 0.14	0.128
Ratio of vertical to the shortest transverse	1.36 ± 0.20	1.33 ± 0.44	1.12 ± 0.25	0.021

presence of air bronchogram on thin-section CT is characteristic of solid adenocarcinoma of the lung. The prognosis of patients with non-small cell lung carcinoma (NSCLC) is better than that of patients with small cell lung cancer (SCLC), and those with NSCLC, while the prognosis of adenocarcinoma with GGO is better than that of NSCLC with a different histology (2). From a pathological point of view, nodules with air bronchogram can represent an intermediate form in the development from GGOs to pure solid lesions. The presence of air bronchogram can therefore be considered as a favorable prognostic factor. Furthermore, if the hypothesis can be confirmed that prognosis of peripheral lung cancer with air bronchogram is not worse than that of nodular GGO or adenocarcinoma of <2 cm, peripheral lung cancer with air bronchogram can be treated with minimally invasive thoracic surgery (MITS), which has the usual advantages of less invasive approaches for patients with lung cancer (30).

We are able to demonstrate that thin-section CT can provide important information for predicting the histology of lung cancer, as well as the prognosis and appropriate treatment methods for patients with peripheral solid lung cancer. Thin-section CT is also useful for reaching a rational histological diagnosis for patients with lung cancer who are not candidates for surgical resection or who are not willing to undergo surgery. To the best of our knowledge, ours is the first report of a systematic evaluation of thin-section CT findings based on histological findings of lung cancer. We were able to confirm that bronchogram is characteristic of solid adenocarcinoma, while other thin-section CT findings are irrelevant for tumor histology and related only to tumor size.

There are a few limitations to our study. First, no patients with large cell carcinoma or adenosquamous carcinoma were included in our study so that the spectrum of disease was not complete. However, such carcinomas actually rarely encounter in a clinical setting. Second, our study was retrospective, which may have resulted in a sampling bias. Third, we could not make a prognostic analysis of air bronchogram for patients with peripheral lung cancer because of our limited clinical data.

In conclusion, air bronchogram on thin-section CT is a characteristic feature of solid adenocarcinoma of the lung. However, other CT findings, including lobulation, coarse spiculation, cavity, pleural tag, density of lobulation, and coarse spiculation, in addition to the ratio of the vertical to the shortest transverse diameter, were found to be unrelated to tumor histology and related only to tumor size.

Funding

This research received no specific grant from any funding agency in the public, commercial, or not-for-profit sectors.

References

1. Jemal A, Siegel R, Xu J, et al. Cancer statistics, 2010. CA Cancer J Clin 2010;60:277–300.
2. SEER cancer statistics review, 1975–2008. See http://seer.cancer.gov/csr/1975_2008/results_merged/sect_15_lung_bronchus.pdf
3. Travis WD, Brambilla E, Noguchi M, et al. International association for the study of lung cancer/american thoracic society/european respiratory society international multidisciplinary classification of lung adenocarcinoma. J Thorac Oncol 2011;6:244–285.
4. Ko JP. Lung nodule detection and characterization with multi-slice CT. J Thorac Imaging 2005;20:196–209.
5. Ettinger DS, Bepler G, Bueno R, et al. Non-small cell lung cancer clinical practice guidelines in oncology. J Natl Compr Canc Netw 2006;4:548–482.
6. Johnson BE, Crawford J, Downey RJ, et al. Small cell lung cancer clinical practice guidelines in oncology. J Natl Compr Canc Netw 2006;4:602–622.
7. Goo JM, Park CM, Lee HJ. Ground-glass nodules on chest CT as imaging biomarkers in the management of lung adenocarcinoma. Am J Roentgenol 2011;196:533–543.
8. Hansell DM, Bankier AA, MacMahon H, et al. Fleischner Society: glossary of terms for thoracic imaging. Radiology 2008;246:697–722.
9. Kuriyama K, Seto M, Kasugai T, et al. Ground-glass opacity on thin-section CT: value in differentiating subtypes of adenocarcinoma of the lung. Am J Roentgenol 1999;173:465–469.
10. Aoki T, Tomoda Y, Watanabe H, et al. Peripheral lung adenocarcinoma: correlation of thin-section CT findings with histologic prognostic factors and survival. Radiology 2001;220:803–809.
11. Tsuchiya R. Implication of the CT characteristics of subcentimeter pulmonary nodules. Semin Thorac Cardiovasc Surg 2005;17:107–109.
12. Park CM, Goo JM, Lee HJ, et al. Nodular ground-glass opacity at thin-section CT: histologic correlation and evaluation of change at follow-up. Radiographics 2007;27:391–408.
13. Godoy MC, Naidich DP. Subsolid pulmonary nodules and the spectrum of peripheral adenocarcinomas of the lung: recommended interim guidelines for assessment and management. Radiology 2009;253:606–622.
14. Lee HY, Lee KS. Ground-glass opacity nodules: histopathology, imaging evaluation, and clinical implications. J Thorac Imaging 2011;26:106–18.
15. Akata S, Yoshimura M, Nishio R, et al. High-resolution computed tomographic findings of small peripherally located squamous cell carcinoma. Clin Imaging 2008;32:259–263.
16. Hashimoto M, Miyauchi T, Heianna J, et al. Accurate diagnosis of peripheral small cell lung cancer with

computed tomography. Tohoku J Exp Med 2009;217:217–221.
17. Oshiro Y, Kusumoto M, Matsuno Y, et al. CT findings of surgically resected large cell neuroendocrine carcinoma of the lung in 38 patients. Am J Roentgenol 2004;182:87–91.
18. Yu JQ, Yang ZG, Austin JH, et al. Adenosquamous carcinoma of the lung: CT-pathological correlation. Clin Radiol 2005;60:364–369.
19. Bland JM, Altman DG. Measuring agreement in method comparison studies. Stat Methods Med Res 1999;8:135–160.
20. Blum A, Feldmann L, Bresler F, et al. Value of calculation of the kappa coefficient in the evaluation of an imaging method. J Radiol 1995;76:441–443.
21. Hansell DM, Bankier AA, MacMahon H, et al. Fleischner Society: glossary of terms for thoracic imaging. Radiology 2008;246:697–722.
22. Naidich DP, Sussman R, Kutcher WL, et al. Solitary pulmonary nodules: CT-bronchoscopic correlation. Chest 1988;93:595–598.
23. Takashima S, Maruyama Y, Hasegawa M, et al. CT findings and progression of small peripheral lung neoplasms having a replacement growth pattern. Am J Roentgenol 2003;180:817–826.
24. Kuriyama K, Tateishi R, Doi O, et al. Prevalence of air bronchograms in small peripheral carcinomas of the lung on thin-section CT: comparison with benign tumors. Am J Roentgenol 1991;156:921–924.
25. Kui M, Templeton PA, White CS, et al. Evaluation of the air bronchogram sign on CT in solitary pulmonary lesions. J Comput Assist Tomogr 1996;20:983–986.
26. Choi JA, Kim JH, Hong KT, et al. CT bronchus sign in malignant solitary pulmonary lesions: value in the prediction of cell type. Eur Radiol 2000;10:1304–1309.
27. Zwirewich CV, Vedal S, Miller RR, et al. Solitary pulmonary nodule: high-resolution CT and radiologic-pathologic correlation. Radiology 1991;179:469–476.
28. Meziane MA, Hruban RH, Zerhouni EA, et al. High resolution CT of the lung parenchyma with pathologic correlation. Radiographics 1988;8:27–54.
29. Shimada Y, Yoshida J, Hishida T, et al. Predictive factors of pathologically proven noninvasive tumor characteristics in T1aN0M0 peripheral non-small cell lung cancer. Chest 2012;141:1003–1009.
30. Rocco G, Internullo E, Cassivi SD, et al. The variability of practice in minimally invasive thoracic surgery for pulmonary resections. Thorac Surg Clin 2008;18:235–247.

Shingyoji et al. BMC Cancer 2013, 13:77
http://www.biomedcentral.com/1471-2407/13/77

BMC Cancer

RESEARCH ARTICLE Open Access

The significance and robustness of a plasma free amino acid (PFAA) profile-based multiplex function for detecting lung cancer

Masato Shingyoji[1*], Toshihiko Iizasa[1], Masahiko Higashiyama[2], Fumio Imamura[3], Nobuhiro Saruki[4], Akira Imaizumi[5*], Hiroshi Yamamoto[5], Takashi Daimon[6], Osamu Tochikubo[7], Toru Mitsushima[8], Minoru Yamakado[9] and Hideki Kimura[1]

Abstract

Background: We have recently reported on the changes in plasma free amino acid (PFAA) profiles in lung cancer patients and the efficacy of a PFAA-based, multivariate discrimination index for the early detection of lung cancer. In this study, we aimed to verify the usefulness and robustness of PFAA profiling for detecting lung cancer using new test samples.

Methods: Plasma samples were collected from 171 lung cancer patients and 3849 controls without apparent cancer. PFAA levels were measured by high-performance liquid chromatography (HPLC)–electrospray ionization (ESI)–mass spectrometry (MS).

Results: High reproducibility was observed for both the change in the PFAA profiles in the lung cancer patients and the discriminating performance for lung cancer patients compared to previously reported results. Furthermore, multivariate discriminating functions obtained in previous studies clearly distinguished the lung cancer patients from the controls based on the area under the receiver-operator characteristics curve (AUC of ROC = 0.731 ~ 0.806), strongly suggesting the robustness of the methodology for clinical use. Moreover, the results suggested that the combinatorial use of this classifier and tumor markers improves the clinical performance of tumor markers.

Conclusions: These findings suggest that PFAA profiling, which involves a relatively simple plasma assay and imposes a low physical burden on subjects, has great potential for improving early detection of lung cancer.

Keywords: Plasma, Amino acid, Lung cancer, Early detection

Background

Several minimally invasive, easy-to-use cancer diagnostic methods using peripheral blood samples have recently been developed to ease the physical burden on patients and to reduce cost and time [1-3]. Computer-aided systems for data mining, (e.g., using multivariate analysis) are now readily available and have shown promising results when applied to metabolic profiles for diagnostic and clinical use [4-6]. Several applications using metabolome analysis based on machine learning to diagnose human cancer using peripheral blood or urine have recently been demonstrated [7-12].

Among metabolites, amino acids are one of the most suitable candidates for focused metabolomics because they are either ingested or synthesized endogenously and play essential physiological roles both as basic metabolites and metabolic regulators. To measure amino acids, plasma free amino acids (PFAAs), which are abundant in the circulation and link all organ systems, are favorable targets because PFAA profiles are influenced by metabolic variations in specific organ systems induced by specific diseases [13-18]. Furthermore, several investigators have reported changes in PFAA profiles in cancer patients, including lung cancer patients [19-27]. However, several discrepancies exist

* Correspondence: mshingyoji@chiba-cc.jp; akira_imaizumi@ajinomoto.com
[1]Division of Thoracic Diseases, Chiba Cancer Center, 666-2, Nitona-cho, Chuo-ku, Chiba 260-8717, Japan
[5] Institute for Innovation, Ajinomoto, CO., Inc, 1-1, Suzuki-cho, Kawasaki-ku, Kawasaki 210-8681, Japan
Full list of author information is available at the end of the article

between the results of these studies due to the limited size of the data set [22].

High-throughput techniques using high-performance liquid chromatography (HPLC)– electrospray ionization (ESI)–mass spectrometry (MS) to measure amino acids with sufficient accuracy for clinical use have also recently been developed [28-31].

By combining these technologies, we recently obtained preliminary data on the efficacy of a diagnostic index based on PFAA concentrations, known as the "Amino-Index technology", which compresses multidimensional information from PFAA profiles into a single dimension and maximizes the differences between patients and controls. This technology was shown to be useful in the early detection of colorectal, breast, and lung cancers in approximately 150 samples from a single medical institute [32,33]. Furthermore, we also verified the efficacy and statistical robustness of this method using larger sample sizes from multiple medical institutes and developed discriminating functions to detect five types of cancer, including lung, gastric, colorectal, breast, and prostate cancer [34,35]. We also found that changes in PFAA profiles that were common to all types of cancer as well as those specific to individual cancers [34] .These functions are used in the "AminoIndex® Cancer Screening" service in Japan.

Lung cancer has been the leading cause of cancer death since 1998, and in Japan, >60,000 patients have died from lung cancer since 2005 [36]. Conventionally, chest X-rays and sputum cytology are used to screen for lung cancer in patients in Japan. However, neither chest X-rays nor sputum cytology are ideal or versatile enough to detect early lung cancer. Although chest X-rays are useful for detecting peripheral lung cancer, this method is not always suitable for early detection [37]. In addition, this technique requires highly skilled technicians to achieve sufficient accuracy. Sputum cytology has been reported to be useful only for the detection of squamous cell carcinoma and is inadequate for detecting adenocarcinoma (which is the major histological type of lung cancer in Japan) or for detecting lung cancer in asymptomatic non-smokers [37].

Compared to chest X-ray and sputum cytology, a PFAA-based diagnostic method would be easier to use because it involves a relatively simple plasma assay, imposes a lower physical burden on patients and does not require advanced technical skills. Moreover, this method can also detect lung cancer regardless of cancer stage and histological type, including small cell lung cancer [32,34,35].

In this study, we aimed to verify the usefulness of PFAA profiling for lung cancer detection using samples that had never been used as a data set to derive discriminating functions. As a result, highly reproducible results were observed in both the PFAA profiles and the discriminating performance of previously obtained PFAA-based, multiplex discriminant functions, suggesting the robustness of PFAA profiling for the early detection of lung cancer.

Methods

Ethics

The study was conducted in accordance with the Declaration of Helsinki, and the protocol was approved by the ethics committees of the Chiba Cancer Center, the Osaka Medical Center for Cancer and Cardiovascular Diseases, the Gunma Prefectural Cancer Center, the Kanagawa Health Service Association, the Kameda Medical Center Makuhari, and the Mitsui Memorial Hospital. All subjects gave their written informed consent for inclusion before participating in the study. All data were analyzed anonymously throughout the study.

Subjects

The participants in this study consisted of Japanese patients who had previously been histologically diagnosed with lung cancer at the Chiba Cancer Center (n=171) between 2007 and 2009. Control subjects (n=3849) without apparent cancers who were undergoing comprehensive medical examinations at the Kanagawa Health Service Association, the Kameda Medical Center Makuhari, or the Mitsui Memorial Hospital, Japan between 2008 and 2010 were recruited to participate in the study. Among the participants, 85 cancer patients (P1) and 421 gender- and age-matched controls (C1) were used as the study dataset for two preliminary studies (Table 1) [32,34]. The remaining 86 cancer patients (P2) and 323 gender- and age-matched controls (C2) were used as a test dataset and were not used to derive the discriminating functions in previous studies (Table 1) [32,34]. The remaining 3427 unmatched controls (C3) were also included and were not used to derive the discriminating functions in previous studies (Table 1) [32,34].

Using these subjects, four data sets were evaluated in this study. Dataset 1 includes P1 and C1, Dataset 2 includes P2 and C2, Dataset 3 includes all of the subjects involved in this study (P1, P2, C1, C2, and C3), and Dataset 4 includes all of the patients involved in this study (P1 and P2) (Table 1).

Measurement of plasma amino acid concentration

Blood samples (5 ml) were collected from forearm veins, after overnight fasting, in tubes containing ethylenediaminetetraacetic acid (EDTA; Termo, Tokyo, Japan) and were immediately placed on ice. Plasma was prepared by centrifugation at 3,000 rpm and 4°C for 15 min and stored at −80°C until analysis. The plasma samples were deproteinized using acetonitrile at a final concentration of 80% before measurement. The amino acid concentrations in the plasma were measured by HPLC–ESI–MS followed by precolumn derivatization. The analytical

Table 1 Demographic and clinical characteristics of the subjects

Subjects		Patients		Controls		
Subgroup		P1	P2	C1	C2	C3
Dataset	1	Used		Used		
	2		Used		Used	
	3	Used	Used	Used	Used	Used
	4	Used	Used			
Number	Total	85	86	421	323	3104
	(Male, Female)	(49,36)	(68,18)	(245,176)	(263,60)	(1898,1206)
Age, y	Mean (SD)	65.1 (9.7)	67.8 (8.2)	63.1 (8.7)	61.9 (6.0)	49.4 (8.0)
	Range	30-90	41-83	28-86	37-88	23-67
BMI	Mean (SD)	22.1 (3.7)	22.4 (3.2)	22.8 (3.0)	23.4 (2.9)	23.2 (3.3)
	Range	14.6~31.2	15.7-34.6	14.2-37.1	16.9-35.4	14.8-41.2
Smoking status	Never	26	18	222	139	1865
	Ex	29	36	106	107	434
	Current	29	29	57	62	695
	Unknown	1	3	36	15	110
pStage[a]	I	33	33			
	II	5	5			
	III	27	22			
	IV	20	23			
	Unknown	0	3			
Histology	Adenocarcinoma	59	55			
	Squamous cell carcinoma	13	12			
	Other NSCLC	5	8			
	SCLC	8	11			

a: Cancer stages were determined according to the International Union Against Cancer TNM Classification of Malignant Tumors, 6th Edition [38].

methods used have previously been described [29-31]. Among the 20 genetically encoded amino acids, glutamate (Glu), aspartate (Asp), and cysteine (Cys) were excluded from the analysis because they are unstable in blood. Citrulline (Cit) and ornithine (Orn) were measured instead because they are relatively abundant in blood and are known to play important roles in metabolism. The following 19 amino acids were measured and analyzed: alanine (Ala), arginine (Arg), asparagine (Asn), Cit, glutamine (Gln), glycine (Gly), histidine (His), isoleucine (Ile), leucine (Leu), lysine (Lys), methionine (Met), Orn, phenylalanine (Phe), proline (Pro), serine (Ser), threonine (Thr), tryptophan (Trp), tyrosine (Tyr), and valine (Val). The concentrations of amino acids in the plasma were expressed as μM values. For analysis of the PFAA profile, two measurements were conducted for each of the 19 amino acids. The absolute concentration of each amino acid and the ratios of the amino acid concentrations expressed by the follow equation as previously described were used [32,34]. The concentrations of the amino acids in the plasma were expressed in μM, and the ratios of the amino acid concentrations were expressed by the follow equation:

$$X2_{i,j} = \frac{X_{i,j}}{\sum_k X_{i,k}}$$

where $X2_{ij}$ is the ratio of the amino acid concentration of the j-th amino acid of the i-th subject, and X_{ij} is the plasma concentration (μM) of the j-th amino acid of the i-th subject.

Measurement of tumor markers

Using serum samples from lung cancer patients, the levels of the following five tumor markers were measured: CEA (chemiluminescence immunoassay, normal range ≦ 5.0 ng/ml), CYFRA (electrochemiluminescence immunoassay, normal range ≦ 3.5 ng/ml), ProGRP (enzyme-linked immunoadsorbent assay, normal range ≦ 46 pg/ml), SCC (enzyme immunoassay, normal range ≦ 1.5 ng/ml), and NSE (radioimmunoassay, normal range ≦ 10 ng/ml) [39].

Calculation of discriminant scores

The PFAA profiles of subjects were substituted into the discriminating functions obtained from the results of

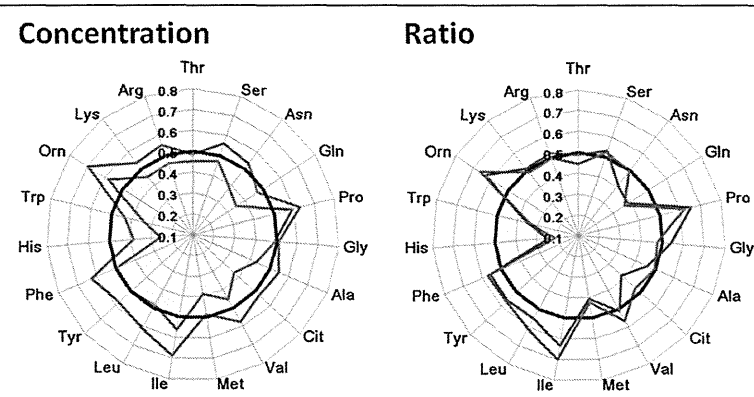

Figure 1 PFAA profiles of lung cancer patients. Axes show the AUC of the ROC for each amino acid to discriminate lung cancer patients from controls. Black bold lines indicate the point at which the AUC of the ROC = 0.5.

three independent preliminary studies [32,34,35]. Both Discriminant- 1 and Discriminant- 3 were logistic regression functions, whereas Discriminant- 2 was a linear discriminating function using plasma concentrations (expressed in μM) as explanatory variables.

Statistical analysis

Mean and SD

The mean amino acid concentrations ± standard deviations (SD) were calculated to determine the overall PFAA profiles for both patients and controls.

Mann–Whitney U-test

The Mann–Whitney *U*-test was used to evaluate differences in the PFAA profiles between the patient and control samples.

ROC curve analysis

Receiver-operator characteristic (ROC) curve analyses were performed to determine the abilities of both the PFAA concentrations and discriminating scores to discriminate between patients and controls. The patient labels were fixed as positive class labels. The 95% confidence interval (95% CI) for the AUC of ROC for the discrimination of patients based on amino acid concentrations and ratios was also estimated as described by Hanley and McNeil [40].

Pearson's correlation coefficients

Pearson's correlation coefficients were calculated among three kinds of discriminant scores (obtained from Discriminant- 1, Discriminant- 2, and Discriminant- 3) using Dataset 3. In addition, coefficients were also calculated using stratified data (patients and controls).

Determination of sensitivity

The cutoff value for Discriminant- 3 was previously determined so that 95% specificity would be obtained [35]. The sensitivity of Discriminant- 3 was also calculated as the ratio of true positives to the summation of the true positives and false negatives. For tumor markers, sensitivities were also determined as the ratio of the number of subjects in which the marker levels were higher than the previously determined normal range to the number of measured subjects.

McNemar test

The McNemar test was performed to evaluate the improvement in sensitivities through combinatorial use of both Discriminant- 3 and the tumor markers.

Software

All of the analyses were performed using MATLAB (The Mathworks, Natick, MA) and GraphPad Prism (GraphPad Software, La Jolla, CA).

Results

Characteristics of the patients and control subjects

Table 1 summarizes the characteristics of the subjects in this study. No significant differences in body mass index (BMI) were observed between patients and matched controls (Table 1). Weight loss due to malnutrition was therefore not expected to influence the results. Although significant differences in average age were observed between the data sets, the effects appeared to be relatively minor because the absolute values of these differences were small (Table 1). Disease stages were determined according to the Sixth Edition of the International Union Against Cancer (UICC) Tumor–Node–Metastasis (TNM) Classification of Malignant Tumors [38]. The fractions of patients at each stage according to the type of cancer were as follows: ~40% stage I, ~5% stage II, ~30% stage III, and ~25% stage IV (Table 1).

The cancer patients were also further subdivided based on histological tumor type; approximately 65% of the patients were classified as having adenocarcinoma, 15%

Table 2 PFAA profiles of controls and lung cancer patients

A. Concentration

Amino acids	P1		C1				P2		C2			
	Mean	SD	Mean	SD	AUC[a]		Mean	SD	Mean	SD	AUC[a]	p[b]
Thr	115.8	30.8	118.5	23.6	0.453		122.6	32.0	121.8	25.8	0.483	
Ser	107.8	20.8	108.8	18.1	0.472		110.7	20.1	106.7	17.4	0.560	
Asn	42.6	7.3	45.2	6.5	0.383	p<0.001	47.9	11.2	46.1	6.5	0.533	
Gln	547.4	71.4	586.9	64.2	0.347	p<0.001	577.5	84.1	587.1	61.5	0.470	
Pro	141.6	37.1	132.3	38.4	0.588	p<0.05	157.3	48.5	138.6	38.5	0.630	p<0.001
Gly	214.3	66.2	209.7	52.2	0.490		208.0	63.5	203.5	47.9	0.511	
Ala	324.2	84.5	343.1	74.8	0.428	<p0.05	366.5	99.8	353.5	69.7	0.550	
Cit	29.0	8.8	33.0	7.4	0.367	p<0.001	33.3	10.3	32.4	7.1	0.530	
Val	215.1	43.1	220.5	39.7	0.453		242.1	43.2	230.0	37.2	0.578	p<0.05
Met	24.2	5.4	25.8	4.6	0.388	p<0.01	26.9	7.2	26.8	4.1	0.489	
Ile	64.7	16.2	60.8	14.4	0.563		73.9	14.0	64.4	13.1	0.689	p<0.001
Leu	117.6	25.3	118.8	23.8	0.484		135.2	26.3	125.2	21.3	0.610	p<0.01
Tyr	65.9	15.0	65.2	12.5	0.503		71.9	15.9	67.3	10.9	0.579	p<0.05
Phe	59.5	9.9	59.6	9.4	0.496		66.5	12.8	61.3	7.9	0.625	p<0.001
His	69.7	12.5	80.2	9.5	0.255	p<0.001	74.1	15.8	81.2	9.4	0.383	p<0.001
Trp	51.3	11.0	57.0	8.8	0.338	p<0.004	56.4	13.4	59.6	8.9	0.432	
Orn	55.2	13.2	51.7	12.6	0.581	p<0.05	61.7	16.4	51.7	10.4	0.696	p<0.001
Lys	183.9	32.7	189.1	30.4	0.450		195.7	37.7	191.6	27.7	0.535	
Arg	93.1	20.7	95.1	16.8	0.460		100.4	24.7	96.4	15.1	0.551	
B. Ratio												
Thr	4.556	0.887	4.544	0.706	0.488		4.460	0.749	4.590	0.781	0.445	
Ser	4.301	0.765	4.200	0.669	0.528		4.080	0.601	4.044	0.617	0.521	
Asn	1.692	0.218	1.740	0.197	0.408	p<0.01	1.749	0.235	1.742	0.194	0.494	
Gln	21.800	2.097	22.661	2.233	0.383	p<0.001	21.276	2.079	22.253	2.053	0.364	p<0.001
Pro	5.599	1.246	5.049	1.225	0.654	p<0.001	5.756	1.504	5.213	1.211	0.622	p<0.001
Gly	8.543	2.566	8.102	1.994	0.542		7.608	1.872	7.703	1.734	0.477	
Ala	12.715	2.141	13.123	2.156	0.459		13.253	2.380	13.321	2.092	0.499	
Cit	1.150	0.328	1.278	0.288	0.378	p<0.001	1.211	0.311	1.229	0.263	0.469	
Val	8.530	1.294	8.454	1.109	0.510		8.925	1.267	8.696	1.198	0.563	
Met	0.955	0.128	0.990	0.115	0.407	p<0.01	0.979	0.152	1.011	0.108	0.424	p<0.05
Ile	2.558	0.519	2.321	0.405	0.631	p<0.001	2.727	0.441	2.427	0.415	0.698	p<0.001
Leu	4.657	0.760	4.547	0.643	0.551		4.986	0.795	4.731	0.671	0.607	p<0.01
Tyr	2.616	0.495	2.503	0.368	0.560		2.644	0.455	2.543	0.335	0.567	
Phe	2.374	0.370	2.295	0.291	0.557		2.470	0.492	2.322	0.272	0.572	p<0.05
His	2.769	0.395	3.091	0.291	0.245	p<0.001	2.702	0.355	3.074	0.295	0.213	p<0.001
Trp	2.034	0.348	2.197	0.301	0.351	p<0.001	2.057	0.373	2.260	0.313	0.338	p<0.001
Orn	2.195	0.482	1.984	0.413	0.631	p<0.001	2.298	0.674	1.955	0.353	0.662	p<0.001
Lys	7.278	0.809	7.265	0.834	0.507		7.169	0.760	7.241	0.824	0.485	
Arg	3.680	0.568	3.657	0.525	0.519		3.650	0.550	3.645	0.473	0.494	

a: AUC indicates AUC of the ROC curve.
b: *p* value derived from the Mann–Whitney *U*-test.

Table 3 Three discriminating functions and amino acids used in each function

Discriminant	Amino acids incorporated into the model	Reference
1	Ala, Val, Ile, His, Trp, Orn	[32]
2	Ser, Gln Pro, Cit, Val, Ile, Phe, His, Trp, Orn	[34]
3	Ser, Gln, Ala, His, Orn, Lys	[35]

as having squamous cell carcinoma, and 10% as having small cell lung cancer (SCLC) (Table 1).

PFAA profiles of lung cancer patients

First, the PFAA profiles of the study data set in previous studies and of the test data set, which was never used for analysis, were used to verify the changes in PFAA profiles observed in cancer patients. Interestingly, the PFAA profiles of the test data set were quite similar to those of the study data set, especially for the ratios of the amino acid concentrations (Figure 1 and Table 2), indicating that the alteration in PFAA profiles observed in cancer patients is robust. Significant increases in both the concentration and ratio of Pro and Orn and significant decreases in His were observed in both the study and test data sets compared to controls (Figure 1 and Table 2). The ratios more clearly reflected the alterations in the PFAA profile than the concentrations; the profiles of five additional amino acids were altered in the ratio data (Gln, Met, and His were decreased in patients, and Ile was increased in patients), while significant changes in concentration were detected in only one direction (Figure 1 and Table 2).

Verification of multivariate discriminating functions

We used three different discriminating functions to distinguish lung cancer patients from controls (Table 3). Discriminant 1 was derived from the PFAA profiles of cancer patients recruited from the Osaka Medical Center for Cancer and Cardiovascular Diseases and controls recruited from the Center for Multiphasic Health Testing and Services of the Mitsui Memorial Hospital [32]. Discriminant 2 and Discriminant 3 were derived from patients from the Osaka Medical Center for Cancer and Cardiovascular Diseases, the Chiba Cancer Center, the Kanagawa Cancer Center, and the Gunma Prefectural Cancer Center and controls recruited from the Center for Multiphasic Health Testing and Services of the Mitsui Memorial Hospital, the Kameda Medical Center Makuhari, and the Kanagawa Health Service Association [34,35]. Discriminant 3 is commercially used in the "AminoIndex® Cancer Screening" service in Japan (Ajinomoto, CO., Inc.) [35]. Both Discriminant 1 and Discriminant 3 were logistic regression models, whereas Discriminant 2 was a linear discriminating function. Explanatory variables used in these functions are listed in Table 3.

Table 4 AUCs of the ROC and the 95% confidential intervals (95% CIs) for each model

	Discriminant-1		Dinscriminant-2		Discriminant-3	
	AUC	95% CI	AUC	95% CI	AUC	95% CI
Dataset 1	0.731	0.668-0.794	0.822	0.768-0.875	0.777	0.718-0.836
Dataset 2	0.797	0.738-0.856	0.775	0.714-0.836	0.761	0.700-0.823
Dataset 3	0.805	0.767-0.846	0.806	0.767-0.843	0.795	0.755-0.831

Three different data sets (Dataset 1, Dataset 2, and Dataset 3) were used to verify the performance of the discriminating functions (Table 4 and Figure 2). Notably, the discrimination abilities of each data set were evaluated using the AUC of the ROC of the discriminate score and were found to be > 0.7 in all cases, indicating that the discrimination functions were both reproducible and robust using independent data sets (Figure 2, Table 4). Specifically, AUCs for the discrimination of lung cancer patients were estimated as follows: 0.731 (95% CI: 0.668 - 0.794) for Dataset 1, 0.822 (95% CI: 0.768 - 0.875) for Dataset 2, and 0.777 (95% CI: 0.718 - 0.836) for Dataset 3 for Discriminant- 1; 0.797 (95% CI: 0.738 - 0.856) for Dataset 1, 0.775 (95% CI: 0.714 - 0.836) for Dataset 2, and 0.761 (95% CI: 0.700 - 0.823) for Dataset 3 for Discriminant 2; and 0.805 (95% CI: 0.767 - 0.846) for Dataset 1, 0.806 (95% CI: 0.767 - 0.843) for Dataset 2, and 0.795 (95% CI: 0.755 - 0.831) for Dataset 3 for Discriminant 3 (Figure 2, Table 4).

Selected explanatory variables partially overlapped for the discriminating functions (Table 3); therefore, the discriminant scores were highly mutually correlated as presented in Table 5. The correlation coefficients were as follows: 0.609 (Discriminant- 1 and Discriminant- 2), 0.552 (Discriminant- 1 and Discriminant- 3), and 0.719 (Discriminant- 2 and Discriminant- 3) for all of the data in Dataset 3. For the patients in Dataset 3 (i.e., P1 and P2), the correlation coefficients were 0.559 (Discriminant- 1 and Discriminant- 2), 0.506 (Discriminant- 1 and Discriminant- 3), and 0.686 (Discriminant- 2 and Discriminant- 3), and the correlation coefficients for the controls in Dataset 3 (i.e., C1, C2, and C3) were 0.674 (Discriminant- 1 and Discriminant- 2), 0.645 (Discriminant- 1 and Discriminant- 3), and 0.810 (Discriminant- 2 and Discriminant- 3) (Table 5).

Combinatorial use of discriminating functions and tumor markers

For further investigation of the clinical applicability of PFAA profiles, the combinatorial use of both the discriminating function from PFAA profiles as explanatory variables and existing tumor markers generally used for lung cancer detection and monitoring (CEA, CYFRA, ProGRP, SCC, and NSE) was assessed [39,41]. In this analysis, Dataset 4 (P1 and P2) was analyzed using discriminant scores obtained from Discriminant- 3. Subgroup analysis was also

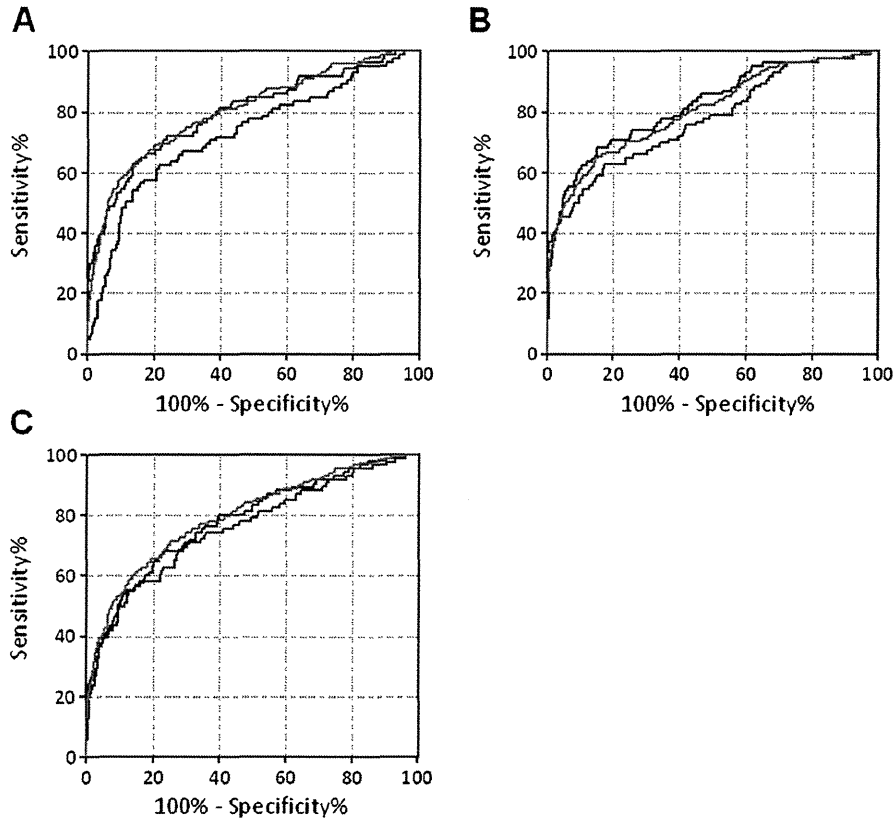

Figure 2 ROC curves of discriminating scores for each discriminating function. Black lines indicate the ROC curves of Dataset 1, blue lines indicate those of Dataset 2, and red lines indicate those of Dataset 3.

performed using patient data stratified into cancer stages (stages I and II). For all patients, significantly higher sensitivities were observed upon combinatorial use of Discriminant- 3 and the tumor markers than upon single use of either Discriminant- 3 or the tumor markers (Figure 3). Similar results were observed among stage I and II patients using the combination of Discriminant- 3 and three tumor markers (CEA, SCC, and NSE), while no significant improvement of sensitivity was observed using Discriminant- 3 and CYFRA or ProGRP (Figure 3). These results suggest that the combinatorial use of Discriminant 3 and other tumor markers is effective for lung cancer detection and monitoring, and an increase in sensitivity was indeed confirmed (Figure 3).

Among the tumor markers, CYFRA and SCC are specific to squamous cell carcinoma (SqCC), ProGRP and NSE are specific to small cell lung cancer (SCLC), and CEA is not specific to any particular histological type of lung cancer [39]. Clinically, the combinatorial use of multiple independent tumor markers is effective for detecting lung cancer. Notably, a low correlation was observed between Discriminant 3 and the tumor markers; the correlation coefficients were 0.304 for CEA, 0.481 for CYFRA, -0.228 for ProGRP, 0.346 for SCC, and 0.102 for NSE (data not shown).

Discussion

In the present study, we verified the usefulness of PFAA profiling for lung cancer detection using new independent samples that had never been used for previous analysis and a derivation of multivariate discriminating function(s) that could distinguish lung cancer patients from control subjects. The results were highly reproducible for the change in PFAA profiles in lung cancer patients and highly discriminatory for lung cancer patients, including those with early stage cancer. Therefore, the results strongly suggest that our method is robust enough for clinical use. Moreover, because our method is a relatively simple plasma assay and imposes minimal physical burden on subjects, our findings suggest that PFAA profiling has great potential for improving the early detection of lung cancer.

Among the three discriminating functions, several amino acids were used in more than one function. His and Orn were incorporated into all of the functions, and Ser, Gln, Ala, Val, Ile, and Trp were incorporated into

Table 5 Correlation coefficients among the discriminant scores of Dataset 3 and its subgroups obtained from three discriminating functions

Compared with;	All data	Patients (P1, P2)	Controls (C1, C2, C3)
Discriminant- 1 and Discriminant- 2	0.609	0.559	0.674
Discriminant- 1 and Discriminant- 3	0.552	0.506	0.645
Discriminant- 2 and Discriminant- 3	0.719	0.685	0.810

two of the three functions (Table 3) [32,34,35]. According to a comparison between the study and test data sets, plasma concentrations of Pro, Ile and Orn were higher in each data set, while the concentrations of Gln, His and Trp were lower (Figure 1 and Table 2). Among these amino acids, changes in the plasma concentrations of four amino acids (Pro, Ile, His, and Orn) were identical to the changes in amino acids in lung cancer patients in previous studies. Maeda et al. have reported that plasma concentrations of Ser, Pro, Gly, Ala, Met, Ile, Leu, Tyr, Phe, Orn, and Lys are increased and His is decreased in lung cancer patients [32]. Miyagi et al. have also reported that the plasma concentrations of Ser, Pro, Gly, Ile, and Orn are increased, whereas Gln, Cit, His, and Trp are decreased in lung cancer patients [34]. Therefore, the results strongly suggest the robustness of these three discriminating functions for the detection of lung cancer.

Moreover, Miyagi et al. have also reported that plasma levels of Gln, Trp, His, Pro, and Orn are commonly altered in cancer patients with five types of cancer (lung cancer, gastric cancer, colorectal cancer, breast cancer, and prostate cancer) [34]. Therefore, the data also strongly suggest that the changes in plasma concentrations of Pro, His, and Orn are essentially associated with carcinogenesis and cancer progression regardless of the location of the tumor.

Although tumor markers have been used extensively to detect lung cancer and estimate clinical condition, the markers are not always useful due to low specificity and insufficient sensitivity. Therefore, combinatorial use of two or more independent tumor markers is necessary for clinical utility [39]. Our results suggest that a PFAA-based diagnostic method would be a novel index to improve the insufficient clinical performance of the tumor markers. Combinatorial use of the tumor markers with

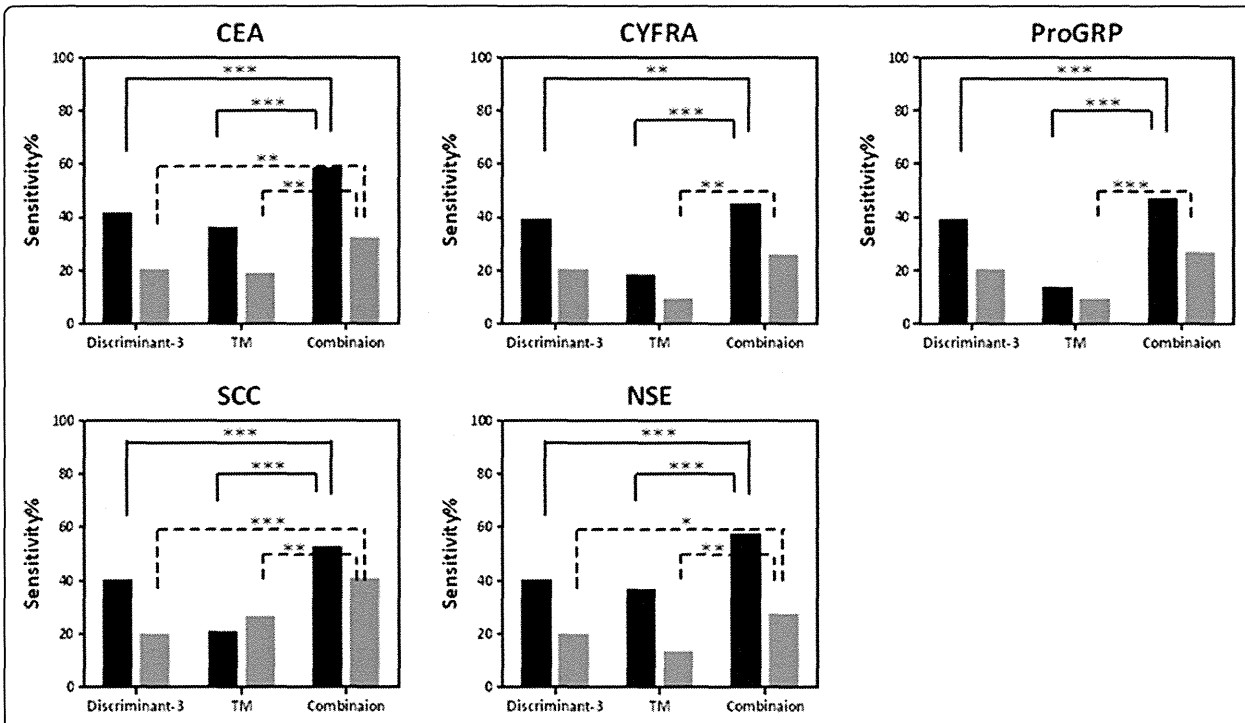

Figure 3 Sensitivities of discriminating scores for Discriminant- 3, levels of tumor markers, and combinatorial use of both markers. Black bars indicate the sensitivities of all of the data from Dataset 4, while gray bars indicate those of patients with stage I and II disease.
* : p<0.05, **: p<0.01, ***: p<0.001 significant at McNemar test.

Discriminant- 3 showed higher sensitivities than any of the tumor markers generally used for lung cancer patients. Additionally, only a low correlation was observed between the discriminating function scores and the tumor marker levels, suggesting the independence of the PFAA profiles from the existing tumor markers. Miyagi et al. have suggested that the change in the PFAA profile in cancer patients reflects two aspects: metabolic changes common to many cancers and metabolic characteristics specific to each cancer [34]. Indeed, although the results were preliminary, the same study demonstrated the possibility of discriminating the cancer type. To clarify this hypothesis, testing the behavior of the discriminating function scores in lung cancer patients after surgery and chemotherapy and in those with recurrence would be necessary.

Because this study was designed as a case–control study, the results cannot be directly applied to further observation or prediction. Therefore, additional validation using a larger sample size is necessary to establish the clinical utility of our approach. Nonetheless, we believe that our results strongly suggest the clinical usefulness of the PFAA-based diagnostic method for the detection of lung cancer.

Competing interest

Takashi Daimon, Osamu Tochikubo, and Minoru Yamakado have been consultants for Ajinomoto, Co., Inc. and receive consultancy fees from Ajinomoto, CO., Inc. Akira Imaizumi and Hiroshi Yamamoto are employees of Ajinomoto, CO., Inc. Masato Shingyoji, Toshihiko Iizasa, Masahiko Higashiyama, Fumio Imamura, Nobuhiro Saruki, Osamu Tochikubo, Toru Mitsushima, Minoru Yamakado, and Hideki Kimura have received research grants from Ajinomoto, CO., Inc. Masahiko Higashiyama, Fumio Imamura, Akira Imaizumi, and Hiroshi Yamamoto have applied for patents for plasma amino acid profiling using multivariate analysis as a diagnostic tool for lung cancer (WO2008/016111).

Authors' contributions

AI, HY and HK designed this study. MS, TI, MH, FI, NS, and HK coordinated the study and collected the background data on the patients. HY, OT, TM, and MY also coordinated the study and supervised the collection of control subjects. MS and AI provided data analysis and wrote the manuscript. AI and TD performed statistical analyses. All authors read and approved the final paper.

Acknowledgements

We thank Dr. Hiroshi Miyano, Mr. Takashi Yamamoto, and Ms. Naoko Kageyama for the amino acid analysis, Dr. Katsuhisa Horimoto for help with the statistical analysis, and Ms. Mariko Takasu and Ms. Tomoko Kasakura for help with data acquisition. We also thank all members of the medical staff of the Chiba Cancer Center, the Osaka Medical Center for Cancer and Cardiovascular Diseases, the Gunma Prefectural Cancer Center, the Center for Multiphasic Health Testing and Services of the Mitsui Memorial Hospital, the Kameda Medical Center Makuhari, and the Kanagawa Health Service Association for help with sample collection.

Author details

[1]Division of Thoracic Diseases, Chiba Cancer Center, 666-2, Nitona-cho, Chuo-ku, Chiba 260-8717, Japan. [2]Department of Thoracic Surgery, Osaka Medical Center for Cancer and Cardiovascular Diseases, 1-3-3, Nakamichi, Higashinari-ku, Osaka 537-8511, Japan. [3]Department of Pulmonary Oncology, Osaka Medical Center for Cancer and Cardiovascular Diseases, 1-3-3, Nakamichi, Higashinari-ku, Osaka 537-8511, Japan. [4]Department of Anesthesia, Gunma Prefectural Cancer Center, 617-1, Takahayashi-nishicho, Ohta 373-8550, Japan. [5]Institute for Innovation, Ajinomoto, CO., Inc, 1-1, Suzuki-cho, Kawasaki-ku, Kawasaki 210-8681, Japan. [6]Department of Biostatistics, Hyogo College of Medicine, 1-1, Mukogawa-cho, Nishinomiya, Japan. [7]Kanagawa Health Service Association, 58, Nihon-odori, Naka-ku, Yokohama 231-0021, Japan. [8]Department of Gastroenterology, Kameda Medical Center Makuhari, 1-3-CD2, Nakase, Mihama-ku, Chiba 261-8501, Japan. [9]Center for Multiphasic Health Testing and Services, Mitsui Memorial Hospital, 1, Kanda-izumicho, Chiyoda-ku, Tokyo 101-8643, Japan.

Received: 21 November 2012 Accepted: 7 February 2013
Published: 15 February 2013

References

1. Hunter MP, Ismail N, Zhang X, Aguda BD, Lee EJ, Yu L, Xiao T, Schafer J, Lee ML, Schmittgen TD, *et al*: **Detection of microRNA expression in human peripheral blood microvesicles.** *PLoS One* 2008, **3**(11):e3694.
2. Roth C, Kasimir-Bauer S, Pantel K, Schwarzenbach H: **Screening for circulating nucleic acids and caspase activity in the peripheral blood as potential diagnostic tools in lung cancer.** *Mol Oncol* 2011, **5**(3):281–291.
3. Roth C, Rack B, Muller V, Janni W, Pantel K, Schwarzenbach H: **Circulating microRNAs as blood-based markers for patients with primary and metastatic breast cancer.** *Breast Canc Res* 2010, **12**(6):R90.
4. Chadeau-Hyam M, Ebbels TM, Brown IJ, Chan Q, Stamler J, Huang CC, Daviglus ML, Ueshima H, Zhao L, Holmes E, *et al*: **Metabolic profiling and the metabolome-wide association study: significance level for biomarker identification.** *J Proteome Res* 2010, **9**(9):4620–4627.
5. Lee K, Hwang D, Yokoyama T, Stephanopoulos G, Stephanopoulos GN, Yarmush ML: **Identification of optimal classification functions for biological sample and state discrimination from metabolic profiling data.** *Bioinformatics* 2004, **20**(6):959–969.
6. Kim Y, Koo I, Jung BH, Chung BC, Lee D: **Multivariate classification of urine metabolome profiles for breast cancer diagnosis.** *BMC Bioinforma* 2010, **11**(2):S4.
7. Nolen B, Velikokhatnaya L, Marrangoni A, De Geest K, Lomakin A, Bast RC Jr, Lokshin A: **Serum biomarker panels for the discrimination of benign from malignant cases in patients with an adnexal mass.** *Gynecol Oncol* 2010, **117**(3):440–445.
8. Pasikanti KK, Esuvaranathan K, Ho PC, Mahendran R, Kamaraj R, Wu QH, Chiong E, Chan EC: **Noninvasive urinary metabonomic diagnosis of human bladder cancer.** *J Proteome Res* 2010, **9**(6):2988–2995.
9. Qiu Y, Cai G, Su M, Chen T, Zheng X, Xu Y, Ni Y, Zhao A, Xu LX, Cai S, *et al*: **Serum metabolite profiling of human colorectal cancer using GC-TOFMS and UPLC-QTOFMS.** *J Proteome Res* 2009, **8**(10):4844–4850.
10. Qiu Y, Patwa TH, Xu L, Shedden K, Misek DE, Tuck M, Jin G, Ruffin MT, Turgeon DK, Synal S, *et al*: **Plasma glycoprotein profiling for colorectal cancer biomarker identification by lectin glycoarray and lectin blot.** *J Proteome Res* 2008, **7**(4):1693–1703.
11. Rocha CM, Barros AS, Gil AM, Goodfellow BJ, Humpfer E, Spraul M, Carreira IM, Melo JB, Bernardo J, Gomes A, *et al*: **Metabolic profiling of human lung cancer tissue by 1H high resolution magic angle spinning (HRMAS) NMR spectroscopy.** *J Proteome Res* 2010, **9**(1):319–332.
12. Urayama S, Zou W, Brooks K, Tolstikov V: **Comprehensive mass spectrometry based metabolic profiling of blood plasma reveals potent discriminatory classifiers of pancreatic cancer.** *Rapid Commun Mass Spectrom* 2010, **24**(5):613–620.
13. Felig P, Marliss E, Ohman JL, Cahill CF Jr: **Plasma amino acid levels in diabetic ketoacidosis.** *Diabetes* 1970, **19**(10):727–728.
14. Felig P, Wahren J, Raf L: **Evidence of inter-organ amino-acid transport by blood cells in humans.** *Proc Natl Acad Sci USA* 1973, **70**(6):1775–1779.
15. Fischer JE, Funovics JM, Aguirre A, James JH, Keane JM, Wesdorp RI, Yoshimura N, Westman T: **The role of plasma amino acids in hepatic encephalopathy.** *Surgery* 1975, **78**(3):276–290.
16. Fischer JE, Rosen HM, Ebeid AM, James JH, Keane JM, Soeters PB: **The effect of normalization of plasma amino acids on hepatic encephalopathy in man.** *Surgery* 1976, **80**(1):77–91.
17. Kimura T, Noguchi Y, Shikata N, Takahashi M: **Plasma amino acid analysis for diagnosis and amino acid-based metabolic networks.** *Curr Opin Clin Nutr Metab Care* 2009, **12**(1):49–53.
18. Noguchi Y, Zhang QW, Sugimoto T, Furuhata Y, Sakai R, Mori M, Takahashi M, Kimura T: **Network analysis of plasma and tissue amino acids and the generation of an amino index for potential diagnostic use.** *Am J Clin Nutr* 2006, **83**(2):513S–519S.

19. Cascino A, Cangiano C, Ceci F, Franchi F, Mineo T, Mulieri M, Muscaritoli M, Rossi Fanelli F: **Increased plasma free tryptophan levels in human cancer: a tumor related effect?** *Anticancer Res* 1991, **11**(3):1313–1316.
20. Cascino A, Muscaritoli M, Cangiano C, Conversano L, Laviano A, Ariemma S, Meguid MM, Rossi Fanelli F: **Plasma amino acid imbalance in patients with lung and breast cancer.** *Anticancer Res* 1995, **15**(2):507–510.
21. Kubota A, Meguid MM, Hitch DC: **Amino acid profiles correlate diagnostically with organ site in three kinds of malignant tumors.** *Cancer* 1992, **69**(9):2343–2348.
22. Lai HS, Lee JC, Lee PH, Wang ST, Chen WJ: **Plasma free amino acid profile in cancer patients.** *Semin Canc Biol* 2005, **15**(4):267–276.
23. Laviano A, Cascino A, Muscaritoli M, Fanfarillo F, Rossi Fanelli F: **Tumor-induced changes in host metabolism: a possible role for free tryptophan as a marker of neoplastic disease.** *Adv Exp Med Biol* 2003, **527**:363–366.
24. Naini AB, Dickerson JW, Brown MM: **Preoperative and postoperative levels of plasma protein and amino acid in esophageal and lung cancer patients.** *Cancer* 1988, **62**(2):355–360.
25. Norton JA, Gorschboth CM, Wesley RA, Burt ME, Brennan MF: **Fasting plasma amino acid levels in cancer patients.** *Cancer* 1985, **56**(5):1181–1186.
26. Proenza AM, Oliver J, Palou A, Roca P: **Breast and lung cancer are associated with a decrease in blood cell amino acid content.** *J Nutr Biochem* 2003, **14**(3):133–138.
27. Vissers YL, Dejong CH, Luiking YC, Fearon KC, von Meyenfeldt MF, Deutz NE: **Plasma arginine concentrations are reduced in cancer patients: evidence for arginine deficiency?** *Am J Clin Nutr* 2005, **81**(5):1142–1146.
28. Fontana S, Alessandro R, Barranca M, Giordano M, Corrado C, Zanella-Cleon I, Becchi M, Kohn EC, De Leo G: **Comparative proteome profiling and functional analysis of chronic myelogenous leukemia cell lines.** *J Proteome Res* 2007, **6**(11):4330–4342.
29. Shimbo K, Kubo S, Harada Y, Oonuki T, Yokokura T, Yoshida H, Amao M, Nakamura M, Kageyama N, Yamazaki J, *et al*: **Automated precolumn derivatization system for analyzing physiological amino acids by liquid chromatography/mass spectrometry.** *Biomed Chromatogr* 2009, **24**(7):683–691.
30. Shimbo K, Oonuki T, Yahashi A, Hirayama K, Miyano H: **Precolumn derivatization reagents for high-speed analysis of amines and amino acids in biological fluid using liquid chromatography/electrospray ionization tandem mass spectrometry.** *Rapid Commun Mass Spectrom* 2009, **23**(10):1483–1492.
31. Shimbo K, Yahashi A, Hirayama K, Nakazawa M, Miyano H: **Multifunctional and highly sensitive precolumn reagents for amino acids in liquid chromatography/tandem mass spectrometry.** *Anal Chem* 2009, **81**(13):5172–5179.
32. Maeda J, Higashiyama M, Imaizumi A, Nakayama T, Yamamoto H, Daimon T, Yamakado M, Imamura F, Kodama K: **Possibility of multivariate function composed of plasma amino acid profiles as a novel screening index for non-small cell lung cancer: a case control study.** *BMC Canc* 2010, **10**(1):690.
33. Okamoto N, Miyagi Y, Chiba A, Akaike M, Shiozawa M, Imaizumi A, Yamamoto H, Ando T, Yamakado M, Tochikubo O: **Diagnostic modeling with differences in plasma amino acid profiles between non-cachectic colorectal/breast cancer patients and healthy individuals.** *Int J Med Med Sci* 2009, **1**(1):1–8.
34. Miyagi Y, Higashiyama M, Gochi A, Akaike M, Ishikawa T, Miura T, Saruki N, Bando E, Kimura H, Imamura F, *et al*: **Plasma free amino acid profiling of five types of cancer patients and its application for early detection.** *PLoS One* 2011, **6**(9):e24143.
35. Okamoto N: **Cancer screening using "AminoIndex Technology".** *Ningen Dock* 2011, **26**(3):454–466.
36. Asamura H, Goya T, Koshiishi Y, Sohara Y, Eguchi K, Mori M, Nakanishi Y, Tsuchiya R, Shimokata K, Inoue H, *et al*: **A Japanese Lung Cancer Registry study: prognosis of 13,010 resected lung cancers.** *J Thorac Oncol* 2008, **3**(1):46–52.
37. Sumitani M, Takifuji N, Nanjyo S, Imahashi Y, Kiyota H, Takeda K, Yamamoto R, Tada H: **Clinical relevance of sputum cytology and chest X-ray in patients with suspected lung tumors.** *Intern Med* 2008, **47**(13):1199–1205.
38. Sobin L, Wittekind C: *TNM Classification of Malignant Tumours, Sixth Edition.* New York: Wiley-Liss; 2002.
39. Ando S, Kimura H, Iwai N, Kakizawa K, Shima M, Ando M: **The significance of tumour markers as an indication for mediastinoscopy in non-small cell lung cancer.** *Respirology* 2003, **8**(2):163–167.
40. Hanley JA, McNeil BJ: **The meaning and use of the area under a receiver operating characteristic (ROC) curve.** *Radiology* 1982, **143**(1):29–36.
41. Molina R, Auge JM, Filella X, Vinolas N, Alicarte J, Domingo JM, Ballesta AM: **Pro-gastrin-releasing peptide (proGRP) in patients with benign and malignant diseases: comparison with CEA, SCC, CYFRA 21–1 and NSE in patients with lung cancer.** *Anticancer Res* 2005, **25**(3A):1773–1778.

doi:10.1186/1471-2407-13-77
Cite this article as: Shingyoji *et al.*: The significance and robustness of a plasma free amino acid (PFAA) profile-based multiplex function for detecting lung cancer. *BMC Cancer* 2013 13:77.

Spheroid Culture of Primary Lung Cancer Cells with Neuregulin 1/HER3 Pathway Activation

Hiroko Endo, BPHRM, Jiro Okami, MD, PhD,† Hiroaki Okuyama, MD, PhD,*§ Toru Kumagai, MD, PhD,‡ Junji Uchida, MD, PhD,‡ Jumpei Kondo, MD, PhD,‖ Tetsuo Takehara, MD, PhD,‖ Yasuko Nishizawa, MD, PhD,§ Fumio Imamura, MD, PhD,‡ Masahiko Higashiyama, MD, PhD,† and Masahiro Inoue, MD, PhD*¶*

Introduction: Primary culture of cancer cells is expected to be useful for investigating the biology of cancer and predicting chemosensitivity for individual patients, yet has been hampered by technical difficulties. We recently developed the cancer tissue–originated spheroid (CTOS) method for the primary culture of colorectal cancer cells. In the present study, we applied this system to the primary culture of non–small-cell lung cancer.

Methods: We used 125 surgical specimens and 18 pleural effusions for CTOS preparation. Partially digested tumor fragments were cultured in a medium for embryonic stem cells. CTOSs were subjected to sensitivity assay and signal transduction assay for the epidermal growth factor receptor (*EGFR*) tyrosine kinase inhibitor (TKI) erlotinib. We also investigated the effects of growth factors in culturing lung cancer CTOS.

Results: The success rate of CTOS preparation from surgical specimens was 80.0%. The CTOS method was also suitable for culturing tumor spheroids from pleural effusions. CTOSs from lung cancer consisted mostly of pure cancer cells. CTOSs and CTOS-derived xenografts retained the characteristics of the original tumors. In vitro assay results showed that *EGFR* mutation status and expression levels corresponded with erlotinib sensitivity, confirming previous clinical findings. Furthermore, we found that neuregulin 1, a ligand of HER3, potently induced CTOS growth.

Conclusions: The CTOS method enables us to obtain primary lung tumor cells of high viability and purity. CTOS could be a new platform for studying lung cancer biology.

Key Words: Primary culture, Non–small-cell lung cancer, EGFR tyrosine kinase inhibitor, Neuregulin 1, HER3.

(*J Thorac Oncol.* 2013;8: 131–139)

Departments of *Biochemistry, †Thoracic Surgery, ‡Thoracic Oncology, and §Pathology, Osaka Medical Center for Cancer and Cardiovascular Diseases, Osaka, Japan; ‖Department of Gastroenterology and Hepatology, Osaka University Graduate School of Medicine, Suita, Japan; and ¶Department of Clinical and Experimental Pathophysiology, Osaka University, Graduate School of Pharmaceutical Sciences, Suita, Japan.

Disclosure: The authors declare no conflict of interest.

Address for correspondence: Masahiro Inoue, MD, PhD, Department of Biochemistry Osaka Medical Center for Cancer and Cardiovascular Diseases, 1-3-3 Nakamichi, Higashinari-ku, Osaka 537–8511, Japan. E-mail: inoue-ma2@mc.pref.osaka.jp

ISSN: 1556-0864/12/0802-131

Despite constant efforts to improve diagnostics and therapeutics, cancer remains a leading cause of death in developed countries, and pulmonary malignancies are the leading cause of cancer-related death worldwide. Studies have shown that some lung adenocarcinomas are addicted to epidermal growth factor receptor (*EGFR*) signaling, and EGFR tyrosine kinase inhibitors (TKIs) are effective treatment in such cases.[1,2] However, these therapies are challenged by primary and acquired resistance, including additional point mutations[3–5] and alternative pathways that bypass the targets of therapeutic reagents.[6–8] Other ErbB family tyrosine kinase receptors are also involved in non–small-cell lung carcinoma (NSCLC);[9] human epidermal growth factor receptor 3 (HER3) is reportedly involved in the acquired resistance to EGFR TKI, whereas HER2 is overexpressed in 10% to 20% of NSCLC and carrying mutations in approximately 2%.[10,11] Bypassing EGFR signaling can be achieved through HER3 phosphorylation by overexpressed hepatocyte growth factor receptor (MET),[6] or by the induction of HER3 ligand as an autocrine loop.[12] Targeting of HER2 is already in clinical use and that of HER3 is under clinical trial.

Much of the above described data have been obtained through preclinical cancer therapy research performed using cancer cell lines. Although cancer cell lines are originally established from patient tumors, they have adapted to the culture conditions, that is, serum-supplemented medium.[13] Long-term cultivation in serum-containing medium reportedly leads to the accumulation of genetic alterations;[14,15] therefore, it must be considered whether cancer cell lines continue to accurately represent the parental cancer cells.

Nevertheless, primary culture of cancer cells is expected to be useful for investigating cancer biology and predicting chemosensitivity for individual patients. However, it has been hampered by technical difficulties, including poor cell viability, weak growth, and contamination by host cells, especially fibroblasts. We recently reported a novel primary culture system for colorectal cancer.[16] The principle of this method is to retain cell–cell contact during preparation. Tumor biopsy specimens are partially digested into fragments and cultured in a serum-free medium for embryonic stem (ES) cells; within a few hours, the irregularly shaped tumor fragments spontaneously form spheroids, termed cancer tissue–originated spheroids (CTOSs). This CTOS method

enables preparation and culture of multiple spheroids consisting of highly pure and viable colorectal cancer cells.

In the present study, we applied the CTOS method to the primary culture of non–small cell lung cancer (NSCLC). We were able to prepare and culture CTOSs from surgical specimens and pleural effusion. CTOSs from NSCLC showed individual responses to EGFR tyrosine kinase inhibitor in vitro and in vivo. CTOSs were also applicable in a signal transduction assay. Moreover, we identified neuregulin 1 (NRG1, also known as heregulin β1), a ligand for HER3, as a prominent growth factor for CTOS growth.

MATERIALS AND METHODS

CTOS Preparation

Surgical specimens and pleural effusion samples from lung cancer patients were obtained from Osaka Medical Center for Cancer and Cardiovascular Diseases, with the patients' informed consent. Surgically resected tissues were minced with a scalpel into approximately 1-mm^3 pieces, and washed with Hank's balanced salt solution (HBSS, Invitrogen, Carlsbad, CA). Specimens were transferred to a 100-ml glass flask and digested in Dulbecco's Modified Eagle's Medium (DMEM) supplemented with 0.26 U/ml Liberase DH (5401089; Roche, Basel, Switzerland) and 1% PenStrep (Invitrogen), at 37°C for 1 to 2 hours with gentle stirring by a magnetic bar. Digested tissue suspensions were passed through 500-μm and 250-μm metal mesh filters to remove large masses of undigested fragments. Suspensions were further filtered through 100-μm and 40-μm cell strainers (BD FALCON, Franklin Lakes, NJ). Fragments on the cell strainer and cells in the flow-through fractions were collected separately, and were each washed with HBSS and cultured in StemPro hESC medium (GIBCO, Carlsbad, CA) in a non-treated dish (EIKEN, Tokyo, Japan). Pleural effusions were transferred to 50-ml tubes and centrifuged at 200 *g*. Pellets were resuspended in HBSS, filtered through 40-μm cell strainers, and collected and cultured in the same manner as surgical specimens.

Immunohistochemistry

Immunohistochemistry was performed on formalin-fixed, paraffin-embedded tumors and CTOSs. CTOSs were embedded in Matrigel growth factor reduced (GFR) (BD Biosciences, Bedford, MA) before fixation in formalin. Sections were dewaxed, rehydrated, and subjected to antigen retrieval by autoclave incubation in citrate buffer (pH 6.0). The primary antibodies used are listed in the Supplementary text (Supplemental Digital Content, http://links.lww.com/JTO/A386). After secondary antibody incubation, sections were visualized with a fluorescence method or biotin-amplified method (Nova RED, VECTOR, Burlingame, CA).

CTOS Culture

For assessing the effects of growth factors, CTOSs were embedded in Matrigel GFR as described above, and cultured in 100 μl of basal medium containing 10 ng/ml or 100 ng/ml of the following growth factors: NRG1 (Peprotech, Rocky Hill, NJ), Long-IGF1 (Gropep, Thebarton SA, Australia), bFGF (Invitrogen), Activin A (R&D Systems, Minneapolis, MN), or EGF (Invitrogen). Basal medium consisted of DMEM/F12, 2% BSA fraction V, 1× nonessential amino acids, 50 U/ml penicillin, 50 μg/ml streptomycin (all from Invitrogen), 50 μg/ml ascorbic acid (SIGMA, St. Louis, MO), 10 μg/ml human transferrin (SIGMA), 0.1 mM β-mercaptoethanol (Wako, Osaka, Japan), and 1× trace elements A, B, C (Mediatech, Manassas, VA).

For assessment of the inhibitory effect of anti-HER3 antibodies on CTOS growth, CTOSs were embedded in Matrigel GFR as described above, cultured in medium containing 10 ng/ml NRG1 or in StemPro hESC, and treated with anti-HER3 antibody (cloneH3.105.5; Calbiochem, La Jolla, CA) at the indicated doses.

CTOS Sensitivity Assay In Vitro

For the erlotinib sensitivity assay, each CTOS was embedded in a gel droplet of Matrigel GFR, and cultured in StemPro hESC containing erlotinib (Toronto Research Chemicals, North York, ON, Canada) at the indicated doses. CTOSs were exposed to erlotinib for 7 days. CTOS viability was evaluated based on CTOS size at day 7, corrected for the CTOS size at day 0. CTOS size was measured using image analysis software (Image J; National Institutes of Health, Bethesda, MD). Half maximal (50%) inhibitory concentration values were calculated with GraphPad Prism 4 software, using the sigmoidal dose-response function.

Animal Studies

Animal studies were performed in compliance with the guidelines of the institutional animal study committee of Osaka Medical Center for Cancer and Cardiovascular Diseases. Primary xenograft tumors were generated by inoculating small pieces of patient tumors into non-obese diabetic/severe combined immunodeficient (NOD/Scid) mice. One hundred CTOSs were suspended in 50 μl of Matrigel GFR, and transplanted subcutaneously into the flanks of NOD/scid mice. CTOSs prepared from mouse xenografts are designated with the postfix "m" in the figures. Treatment was started when the tumor volume reached approximately 65 mm^3. Erlotinib (Tarceva, CHUGAI Pharmaceutical, Tokyo, Japan) was suspended in 0.5% methyl cellulose, and administered at a dose of 100 mg/kg orally once a day, ×5, for 2 weeks.

Western Blot

CTOSs were cultured overnight in growth factor-free DMEM-F12, and pulsed with StemPro hESC supplement or 10 ng/ml of the indicated growth factors for 15 minutes. CTOSs were lysed with cell lysis buffer (10 mM Tris (pH 7.4), 0.15 M NaCl, 1% NP40, 0.25% sodium deoxycholate, 0.05 M NaF, 2 mM EDTA, 0.1% SDS, 2 mM $NaVO_4$, 10 μg/ml aprotinin, 10 μg/ml leupeptin, and 1 mM PMSF). Western blot was performed as previously described.[17] For signal transduction assays under erlotinib treatment, CTOSs were cultured overnight under growth-factor–starved conditions, incubated for 1 hour with erlotinib, and pulsed with 10 ng/

ml epidermal growth factor (EGF) for 15 minutes. Primary antibodies used are listed in the Supplemental text.

Statistical Analysis

Data are expressed as mean, SD. Statistical analysis was performed using Student's *t* test. Differences were considered significant at *p* values less than 0.05.

RESULTS

Preparation and Characterization of CTOSs from Lung Cancer Patients

To apply the CTOS technology[16] to NSCLC, surgically resected tumor tissues were mechanically minced and enzymatically digested. Samples were then filtered through cell strainers and divided into two fractions: the organoid fraction (tissue fragments on the cell strainer) and the flow-through fraction. The irregular-shaped fragments in the organoid fraction formed spheroids within a few hours in a serum-free medium for ES cell culture (Fig. 1A, Supplementary Fig. 1A, http://links.lww.com/JTO/A355). The flow-through fraction mostly consisted of single cells, small-cell aggregates, and debris; we occasionally found small CTOS-like structures in the flow-through fraction, probably derived from cell aggregates (Supplementary Fig. 1B, http://links.lww.com/JTO/A355). CTOSs were also prepared from pleural effusions, without any dissociation process (Fig. 1B). When CTOSs were dissociated into single cells by trypsin treatment, the dead cells increased over time (Supplementary Fig. 1C, http://links.lww.com/JTO/A355). Thus, retaining cell–cell contact was crucial for preparation and maintenance of viable lung cancer cells, as previously observed in CTOSs of colorectal cancer.[16]

Flow cytometric analysis revealed that CTOSs from adenocarcinoma mostly consisted of epithelial cell adhesion molecule (EpCAM)–positive epithelial cells. CD45-positive hematopoietic cells were barely detectable in CTOSs (Fig. 1C). In contrast, cells in the flow-through fraction consisted of various types of cells, including EpCAM-negative non-epithelial cells and CD45-positive cells (Fig. 1C). Next, we assessed the purity of CTOSs by immunohistochemistry. The original patient tumors consisted of various type of cells, including epithelial cells (E-cadherin positive), myofibroblasts (α-smooth muscle actin [α-SMA] positive), and macrophages (CD68 positive). In contrast, the cells in CTOSs were almost exclusively E-cadherin positive (Fig. 1D). Thus, highly pure epithelial cells could be prepared from bulk tumor tissues by the CTOS method.

CTOSs were successfully prepared from 100 of 125 NSCLC samples (80.0%) from surgically resected tumors, and in eight of 18 pleural effusion samples (44.4%), including all histologic subtypes (Table 1, Supplementary Table 1, Supplemental Digital Content 2, http://links.lww.com/JTO/A356). In most of the failed cases, tumor fragments were not observed in the effusion. CTOSs were also prepared from small-cell lung cancer (Supplementary Table 1, Supplemental Digital Content 2, http://links.lww.com/JTO/A356). CTOSs were successfully prepared from all (5 of 5) primary xenograft

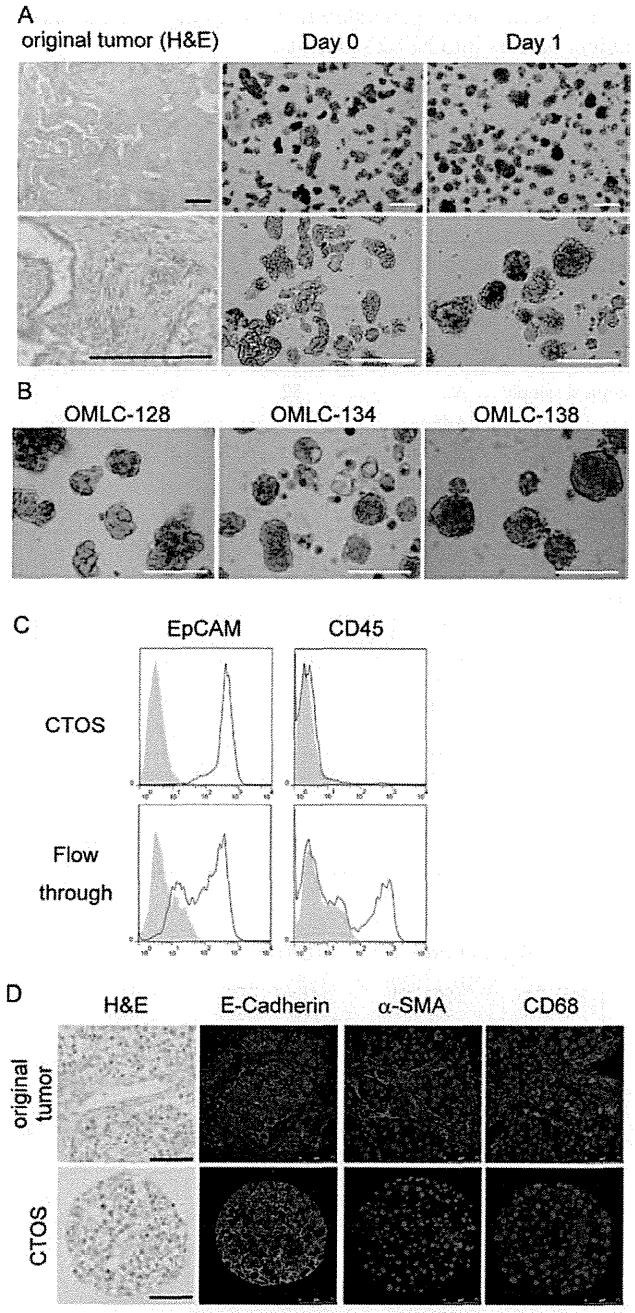

FIGURE 1. Preparation and characterization of CTOSs from patients' lung tumors. *A*, H&E staining of original tumor and phase contrast images of organoid fraction at the indicated times after OMLC-58 preparation. Low- (upper panels) and high-magnification (lower panels) images are shown. Scale bar: 200 μm. *B*, Phase contrast images of CTOSs from three independent pleural effusion samples. Scale bar: 200 μm. *C*, Flow cytometric analysis of the indicated cell-surface antigens by specific antibodies (solid line) or isotype controls (gray filled). *D*, OMLC-40 subjected to H&E staining and immunohistochemistry of E-cadherin (green), α-SMA (red), CD68 (red), and Hoechst33342 (blue). Scale bar: 75 μm. H&E, hematoxylin and eosin.

tumors, which were generated by inoculating small pieces of patient tumors into NOD/scid mice.

CTOS Preserved the Original Tumor Characteristics

To examine the tumorigenic capacity of CTOS, 100 CTOSs (approximately 1×10^4 cells) were transplanted into the flanks of NOD/scid mice. When primary CTOSs prepared from patient tumors were subcutaneously injected into immunodeficient mice, the CTOSs from six of 18 cases (33.3%) formed xenograft tumors (Supplementary Table 1, Supplemental Digital Content 2, http://links.lww.com/JTO/A356). However, CTOSs from primary xenograft tumors formed xenograft tumors in four of five cases (80%). Histologic analysis revealed that CTOSs and mouse xenograft tumors exhibited characteristics of the original patient tumors, at least of some parts in mixed subtype tumors (Fig. 2A). Xenografts or CTOSs also preserved the immunohistochemical characteristics of the original tumors, including staining patterns of EGFR, CK7, TP53, and neural cell adhesion marker (Fig. 2B, Supplementary Fig. 2, Supplemental Digital Content 3, http://links.lww.com/JTO/A357). The ratio of CD133-positive cells, a reported marker of cancer stem cells (CSCs) in lung cancer,[18] was not enriched in CTOSs (Supplementary Fig. 3, Supplemental Digital Content 4, http://links.lww.com/JTO/A358).

TABLE 1. Success Rate of CTOS Formation from Lung Cancer Specimen

		Sample Number	CTOS Formation	Success Rate (%)
Surgical sample	Ad	82	64	78.0
	AdSq	6	6	100
	Sq	31	25	80.6
	Large	4	4	100
	Pleomorphic	2	1	50.0
	Total	125	100	80.0
Pleural effusion	Ad	15	7	47
	AdSq	1	1	100
	Sq	2	0	0
	Total	18	8	44.4
		(8)[a]	(8)[a]	(100)[a]

CTOS, cancer tissue–originated spheroid; Ad, adenocarcinoma; Sq, squamous cell carcinoma; AdSq, adenosquamouse cell carcinoma,; Large, large-cell carcinoma, Pleomorphic, pleomorphic carcinoma.

[a]Excluding samples without any tumor fragments after filtration of the pleural effusion

Response of Lung CTOSs to EGFR TKI

We successfully grew lung CTOSs in vitro in StemPro medium, embedded in Matrigel GFR (Supplementary Fig. 4A, Supplemental Digital Content 5, http://links.lww.com/JTO/A358). Under these culture conditions, 67.2% of CTOSs grew to more than 1.2 times their original size after 7 days (Supplementary Fig. 4B, Supplemental Digital Content 5, http://links.lww.com/JTO/A359). CTOSs from adenocarcinomas tended to grow better compared with those from squamous cell carcinomas.

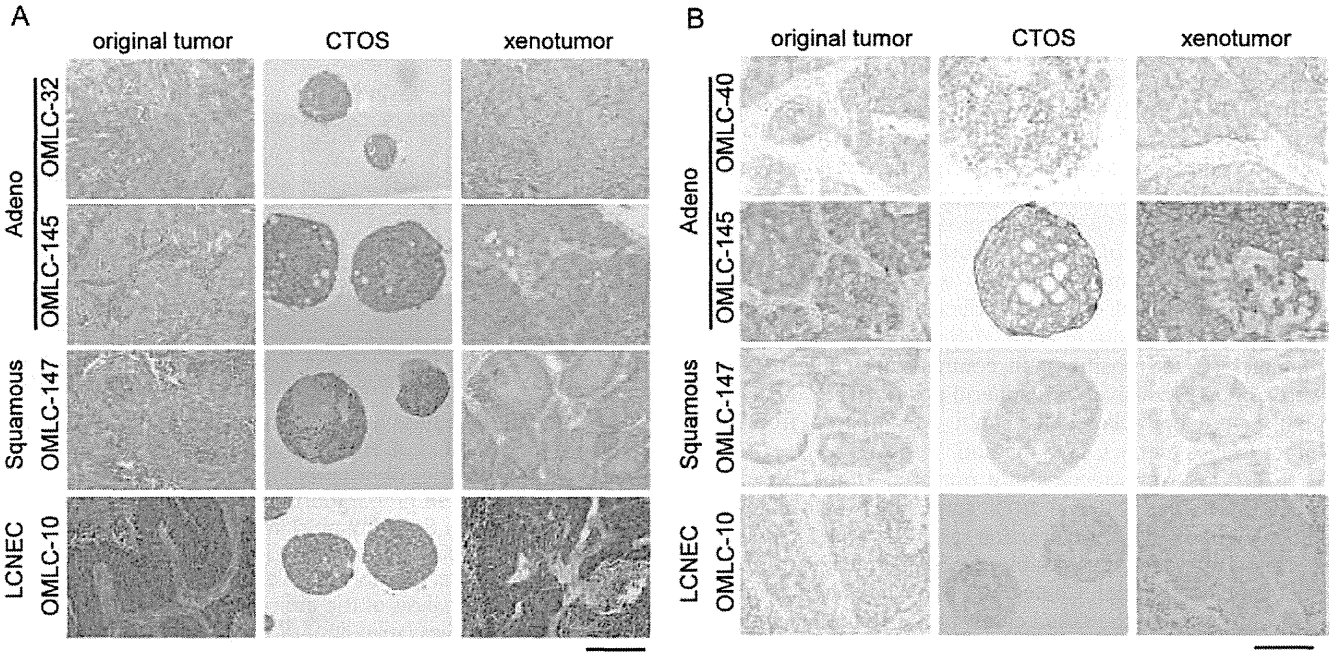

FIGURE 2. CTOS-derived xenotumors preserved the original characteristics of parental tumors. *A*, H&E staining of the indicated cases. *B*, Immunohistochemistry of EGFR from the indicated cases. Original tumor (left column), CTOS (middle column), and xenograft tumor (right column). Adeno, adenocarcinoma; Squamous, squamous cell carcinoma; LCNEC, large-cell neuroendocrine carcinoma. Scale bar: 100 μm.